

Unscented Kalman Filter based State of Charge Estimation for the Equalization of Lithium-ion Batteries on Electrical Vehicles

Yusuf Muratoglu

Department of Electric and Electronic Engineering
Mersin University, Mersin, Turkey
muratoglu.yusuf@gmail.com

Alkan Alkaya

Department of Electric and Electronic Engineering
Mersin University, Mersin, Turkey
alkanalkaya@mersin.edu.tr

Abstract—Accurate state of charge estimation and robust cell equalization are vital in optimizing the battery management system and improving energy management in electric vehicles. In this paper, the passive balance control based equalization scheme is proposed using a combined dynamic battery model and the unscented Kalman filter based state of charge estimation. The lithium-ion battery is modeled with a 2nd order Thevenin equivalent circuit. The combined dynamic model of the lithium-ion battery, where the model parameters are estimated depending on the state of charge, and the unscented Kalman filter based state of charge, are used to improve the performance of the passive balance control based equalization. The experimental results verified the superiority of the combined dynamic battery model and the unscented Kalman filter algorithm with very tight error bounds. Furthermore, these results showed that the presented passive balance control based equalization scheme is suitable for the equalization of series-connected lithium-ion batteries.

Keywords—combined dynamic modelling; li-ion battery; passive balance control; SoC based equalization; SoC estimation; unscented Kalman filter

I. INTRODUCTION

Conventional fossil fuel vehicles are emitting a considerable amount of CO₂. In response to the concern for the protection of environment, automotive industries proposed electrical vehicles (EVs) as a solution for conventional fossil fuel vehicles [1-3]. Rechargeable battery technologies which have become an alternative power are used in the EVs. Batteries with different chemicals such as Ni-based batteries, Li-based batteries, Na-based batteries and Lead Acid batteries are used in EVs. Li-ion batteries are more preferred in electric vehicles due to their significant advantages such as high energy density and nominal cell voltage, long life and having no memory effect [4, 5]. The high performance and safe use of Li-ion batteries depends on the efficiency of their battery management system (BMS). The State of Charge (SoC) of the Li-ion battery, defined as the ratio of the remaining capacity and maximum available capacity of a battery, is a key component of the BMS for the equalization of battery packs on EVs. SoC cannot be measured directly from the battery. Therefore, SoC should be estimated by using an accurate

battery model and measured signals such as current and voltage [6-8].

Modeling of Li-ion battery in EVs applications can be mainly divided into three categories: electrochemical models, mathematical models and electrical equivalent circuit (EEC) models [9]. The complexity of the electrochemical models and the low accuracy of mathematical models led to the investigation of the EEC models. EEC models can be classified based on the different circuit topology used. Partnership for a New Generation of Vehicles (PNGV), Randles, National Renewable Energy Laboratory (NREL) and Thevenin models are the most used electrical circuit models in EV applications [10, 11]. SoC estimation is more powerful with an accurate battery model. There are many methods to estimate the SoC of a Li-ion battery, methods such as coulomb counting (CC), open circuit voltage (OCV), neural network (NN), fuzzy logic, and Kalman filter based algorithms [12-16]. CC method is the basic approach which is widely used for SoC estimation, but it accumulates error problems. In addition, the initial SoC must be known in order to use this method [17, 18]. OCV method is another basic technique which can be used to determine SoC directly, but this method suffers from long resting time [19, 20]. NN and fuzzy logic methods define the battery as a black-box system and can achieve accurate SoC results. However, these methods are in need of a large and of good quality training data set. The model performance strongly depends on the data set used [21, 22]. Kalman filter (KF) which can solve initial SoC and cumulative error problems is widely used as an accurate SoC estimator, but it is only suitable for linear systems [23, 24]. Extended Kalman filter (EKF) known as the nonlinear extension of the conventional KF, is the most commonly used filter to estimate SoC. EKF linearizes the battery model using Taylor series expansion and Jacobian matrix [25]. EKF ensures accurate estimation of the SoC of the battery using the measured load current and terminal voltage. The accuracy of EKF based SoC estimation depends on the precision of the battery model and information of the system noise and covariance matrix [26-28]. However, the EKF has drawbacks. The linearization process using Jacobian matrices could have high computation cost. Unscented Kalman filter (UKF) uses an unscented transformation with a set of sigma points to estimate

SoC without linearization [29]. Due to this transformation, UKF has more robust accuracy than EKF in estimating posterior mean and covariance of the state distribution [30-33]. Changes in internal impedance or capacity reduction due to cell aging cause deviations in cell behavior. Therefore, equalization of the cells in the battery pack is essentially required. Cell equalization can be mainly categorized into SoC based and voltage-based methods [34-36]. In the voltage-based method, the voltage is measured directly on the battery and is easily used in cell equalization. Voltage, which is the external characteristics of the battery cannot reflect the capacity or the internal resistance. Therefore, the voltage-based method is unsuitable for determining the battery imbalance. On the other hand, SoC is affected by both internal and external characteristics of the battery such as battery voltage/current, temperature, internal resistance, and capacity. To improve the cell equalization, the SoC based method is more suitable because SoC represents a comprehensive performance of the battery characteristic [37].

In this study, the second order Thevenin equivalent circuit method is chosen considering optimum model accuracy and complexity. Equivalent circuit parameters are associated with SoC to reflect the dynamic characteristics of the Li-ion battery. The combined dynamic battery model (a combination of Thevenin equivalent circuit model, OCV method and CC method) is used to better represent the dynamical behavior of the Li-ion battery. According to the combined dynamic battery model, UKF based SoC estimation is used to implement the equalization of Li-ion battery packs. In order to protect series-connected Li-ion cells from cell inconsistencies, passive balance control (PBC) is used with SoC based equalization.

II. COMBINED DYNAMIC MODELING OF LI-ION BATTERIES

The dynamic model of the Li-ion battery was formed by combining different methods. The combined dynamic battery model is constructed using second order Thevenin model, OCV method, and CC method. The schematic diagram of the combined dynamic battery model is shown in Figure 1.

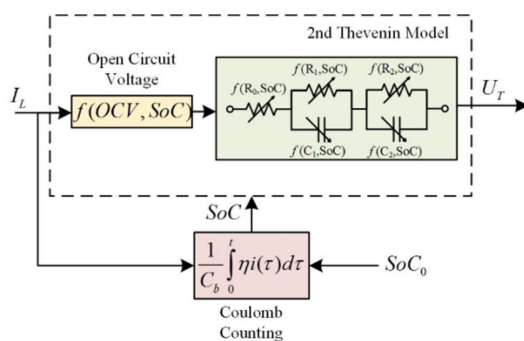


Fig. 1 The schematic diagram of the combined dynamic battery model

SoC is obtained from the load current by using the CC method. The definition of the CC method is:

$$SoC_t = SoC_0 - \frac{1}{C_b} \int_0^t \eta I_{L,\tau} d\tau \quad (1)$$

where SoC_t is the present SoC, SoC_0 is the initial SoC, C_b is the maximum available capacity, η is the charge-discharge efficiency, and $I_{L,\tau}$ is the load current.

The relationship between OCV and SoC is determined by the OCV method. OCV is defined as electrical potential difference between the two terminals of the battery when it is disconnected from the electrical load. OCV has a non-linear relationship with SoC which is obtained by the curve fitting method using the rest points of the OCV of the test data. Second order Thevenin equivalent circuit model, given in Figure 2, is chosen as the cell characteristic of Li-ion battery due to its high precision and low complexity. The equivalent circuit parameters can be changed dynamically depending on SoC.

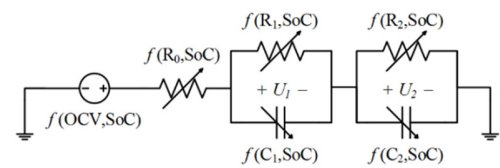


Fig. 2 Second order Thevenin equivalent circuit model

The state-space representation of the combined dynamic battery model is:

$$x = [SoC \quad U_1 \quad U_2]^T \quad (2)$$

$$\dot{x} = \begin{bmatrix} 1 & 0 & 0 \\ 0 & -1/f(R_1, SoC)f(C_1, SoC) & 0 \\ 0 & 0 & -1/f(R_2, SoC)f(C_2, SoC) \end{bmatrix} x + \begin{bmatrix} -\eta/C_b \\ 1/f(C_1, SoC) \\ 1/f(C_2, SoC) \end{bmatrix} I_L \quad (3)$$

$$y = [f(OCV, SoC) \quad -1 \quad -1]x + [-f(R_0, SoC)]I_L \quad (4)$$

where $f(R_0, SoC)$ is the ohmic resistance, $f(R_1, SoC)$ and $f(R_2, SoC)$ are polarization resistances, $f(C_1, SoC)$ and $f(C_2, SoC)$ are polarization capacitances, and U_1 and U_2 are the polarization voltages crossing on C_1 and C_2 .

III. UKF ALGORITHM

UKF is a widely used state estimator for nonlinear systems. The UKF uses the unscented transformation principle rather than linearizing the nonlinear functions as in the EKF. The UKF consists of four major steps: initialization, sigma point calculation, state prediction and measurement update. In the initialization step, mean of initial state \bar{x}_0^s and covariance P_0^s are estimated as Gaussian random vectors:

$$\bar{x}_0^s = E[x_0^s] \quad (5)$$

$$P_0^s = E[(x_0^s - \bar{x}_0^s)(x_0^s - \bar{x}_0^s)^T] \quad (6)$$

Then, s set of sigma points are selected by using unscented transformation principle in sigma point calculation step:

$$\lambda = \alpha^2(N + \kappa) - N \quad (7)$$

$$X_{k,n-1}^s = \begin{cases} \bar{x}_{n-1}^s & k = 0 \\ \bar{x}_{n-1}^s + \sqrt{(N + \lambda)P_{n-1}^s} & k = 1, \dots, N \\ \bar{x}_{n-1}^s - \sqrt{(N + \lambda)P_{n-1}^s} & k = N + 1, \dots, 2N \end{cases} \quad (8)$$

Each sigma point passes through the non-linear functions $f(\cdot)$ and $h(\cdot)$. Priori state estimate $\hat{x}_{n|n-1}$, priori error covariance matrix $P_{n|n-1}$ and measurement of system output vector \hat{y}_{n-1} are calculated in state prediction step:

$$X_{k,n-1}^x = f(X_{k,n-1}^x, X_{k,n-1}^v, u_{n-1}) \quad (9)$$

$$Y_{n|n-1} = h(X_{n|n-1}^x, X_{n-1}^w, u_n) \quad (10)$$

$$\hat{x}_{n|n-1} = \sum_{k=0}^{2N} (w_m^{(k)} X_{k,n|n-1}^x) \quad (11)$$

$$P_{n|n-1} = \sum_{k=0}^{2N} w_c^{(k)} (X_{k,n|n-1}^x - \hat{x}_{n-1}) (X_{k,n|n-1}^x - \hat{x}_{n-1})^T \quad (12)$$

$$\hat{y}_{n-1} = \sum_{k=0}^{2N} (w_m^{(k)} Y_{k,n|n-1}) \quad (13)$$

where the weights of the sigma points are $w_m^{(k)} = \frac{\lambda}{N + \lambda}$ and $w_c^{(k)} = \frac{\lambda}{N + \lambda} + (1 - a^2 + \beta)$ for $k = 0$, $w_m^{(k)} = w_c^{(k)} = \frac{1}{2(N + \lambda)}$ for $k = 1, \dots, 2N$.

Finally, the measurement covariance P_{yn} and the cross-correlation covariance $P_{xn,yn}$ are calculated. Kalman gain K_n is calculated based on measurement covariance and cross-correlation covariance. Posteriori state estimate $\hat{x}_{n|n}$ and posteriori error covariance matrix $P_{n|n}$ are calculated in the measurement update step:

$$P_{yn} = \sum_{k=0}^{2N} w_c^{(k)} (Y_{k,n|n-1} - \hat{y}_{n-1}) (Y_{k,n|n-1} - \hat{y}_{n-1})^T \quad (14)$$

$$P_{xn,yn} = \sum_{k=0}^{2N} w_c^{(k)} (X_{k,n|n-1}^x - \hat{x}_{n-1}) (Y_{k,n|n-1} - \hat{y}_{n-1})^T \quad (15)$$

$$K_n = P_{xn,yn} P_{yn}^{-1} \quad (16)$$

$$\hat{x}_{n|n} = \hat{x}_{n|n-1} + K_n (y_n - \hat{y}_n) \quad (17)$$

$$P_{n|n} = P_{n|n-1} - K_n P_{yn} K_n^T \quad (18)$$

IV. PASSIVE BALANCING CONTROL FOR SOC BASED EQUALIZATION

Battery packs used in EVs, contain many cells. These cells interact with each other. Inconsistencies that may occur in these interacted cells can lead to reduced capacity, overcharge and over-discharge. Cell equalization is essentially required to

prevent cell inconsistencies in the battery pack. Traditionally, PBC is used to protect Li-ion cells from cell inconsistencies with SoC based equalization. The fixed shunting resistor method shown in Figure 3 is one of the most common used in PBC. This method is accomplished by using a switch and drain resistor in parallel with each battery cell.

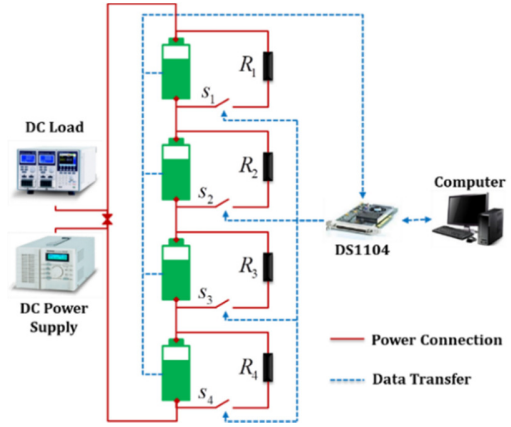


Fig. 3 Schematic diagram of fixed shunting resistor method

V. EXPERIMENTAL VALIDATION

In order to validate the UKF based balancing performance of Li-ion battery packs, an experimental test bench was set up. This test bench consisted of a programmable dc power supply (Gwinstek PSH-3620A), a programmable dc load (Gwinstek PEL-2002/2040), a real-time controller (Dspace DS1104), a Li-ion battery (Panasonic NCR18650B), a balancing circuit and a PC as shown in Figure 4. The balancing circuit shown in Figure 5 is developed to perform SoC based equalization for battery packs by using PBC. The SoC of each cell is compared with the average SoC in the cell balancing circuit. When the difference is over a predetermined threshold of inconsistency, the equalization begins. Otherwise the equalization process stops.

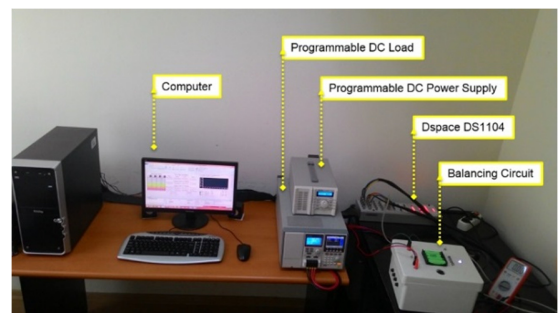


Fig. 4 Experimental test bench

A. Determination of OCV

Impulse discharge test was performed to determine OCV in the experimental test bench. In this test, the Li-ion battery was discharged for 5 minutes and rested for 2 hours. This process continued until the battery was fully discharged. The OCV was obtained using the resting points of the discharge process with the curve fitting method.

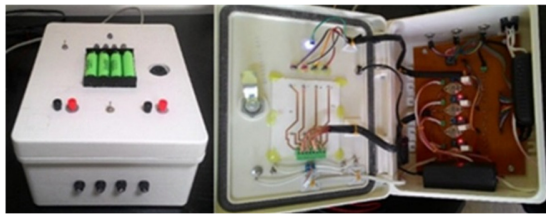


Fig. 5 The balancing circuit

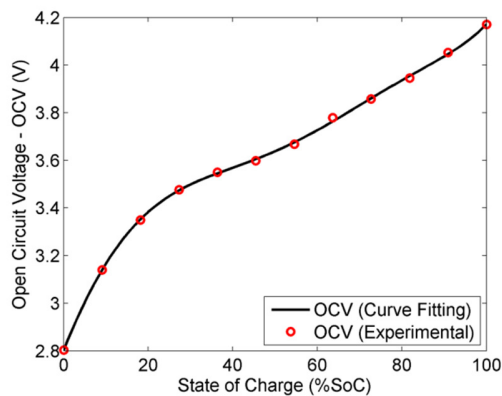


Fig. 6 OCV-SoC non-linear relationship

The OCV curve, given in Figure 6, can be represented with a sixth degree polynomial as:

$$f(U_{OCV}, SoC) = 16.07 \times SoC^6 - 43.57 \times SoC^5 + 37.89 \times SoC^4 - 5.85 \times SoC^3 - 7.59 \times SoC^2 + 4.41 \times SoC + 2.8 \quad (19)$$

B. UKF Based SoC Estimation

UKF algorithm has been tested on the combined dynamic battery model to estimate SoC. The initial parameters of the UKF were defined as: state variable $x_0 = [SoC_0 \ 0 \ 0]^T$, covariance matrix $P = diag(1,1,1)$, weight matrix $Q = diag(10^{-10}, 10^{-10}, 10^{-10})$ and $R = 10$. Q and R weight matrices were determined by trial and error. The SoC_0 was set to 0.8 (80%), in order to better interpret the sensitivity to the initial state of UKF algorithm. SoC estimation performance based on UKF is shown in Figure 7.

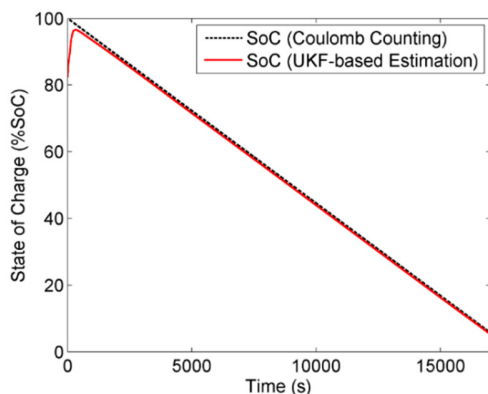


Fig. 7 UKF based SoC estimation

It can be seen that the UKF algorithm can quickly eliminate the initial SoC error and accurately track the SoC after the elimination of the initial error. The calculated estimation error signals are shown in Figure 8 with the initial SoC error. In order to verify the performance of the UKF algorithm, detailed calculations were carried out by using the comparison of the estimation results. It is clear that the UKF algorithm with the combined dynamic battery model provide robust performance in detailed calculations (Table I).

TABLE I. DETAILED CALCULATIONS FOR UKF RESULTS

	Mean Error	Mean square error	Error variance
UKF Results	1.91%	1.6380×10^{-4}	1.0133×10^{-4}

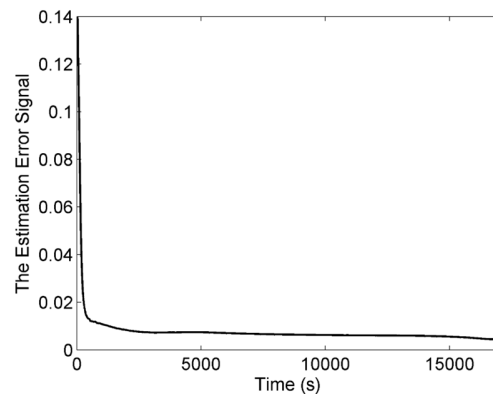


Fig. 8 Error signal of UKF based SoC estimation

C. Real-time User Interface

The interfaces of the battery equalization, shown in Figure 9 and Figure 10 are built in MATLAB/Simulink and DS1104 ControlDesk respectively. The architecture consists of a measurement block, a Li-ion battery block and a cell balancing block. The measurement block captures battery voltages, battery currents and initial SoCs of the individual Li-ion cells. Battery voltage and battery current data of Li-ion battery cells were measured online by using the DS1104 R&D controller board. The initial SoC was determined by the use of these data and CC method. The obtained data were given as input to the Li-ion battery block. The Li-ion battery block estimates SoC by using UKF for the cell balancing block. In the Li-ion battery block, the SoC was estimated with the combined dynamic battery model based on the UKF algorithm. The combined dynamic battery model consists of a second order Thevenin equivalent circuit, OCV, and CC. The cell balancing block keeps the SoC of the cells at the same level with the PBC. The algorithm of the equalization process is given in Figure 11. Voltage and current of the Li-ion cells were obtained. The initial SoC of each Li-ion cell was determined by the OCV method. The SoC of each Li-ion cell was estimated and compared with the average SoC. When the SoC difference of each Li-ion cells was over the predetermined threshold of inconsistency, the balancing switch turned on, otherwise it stayed off.

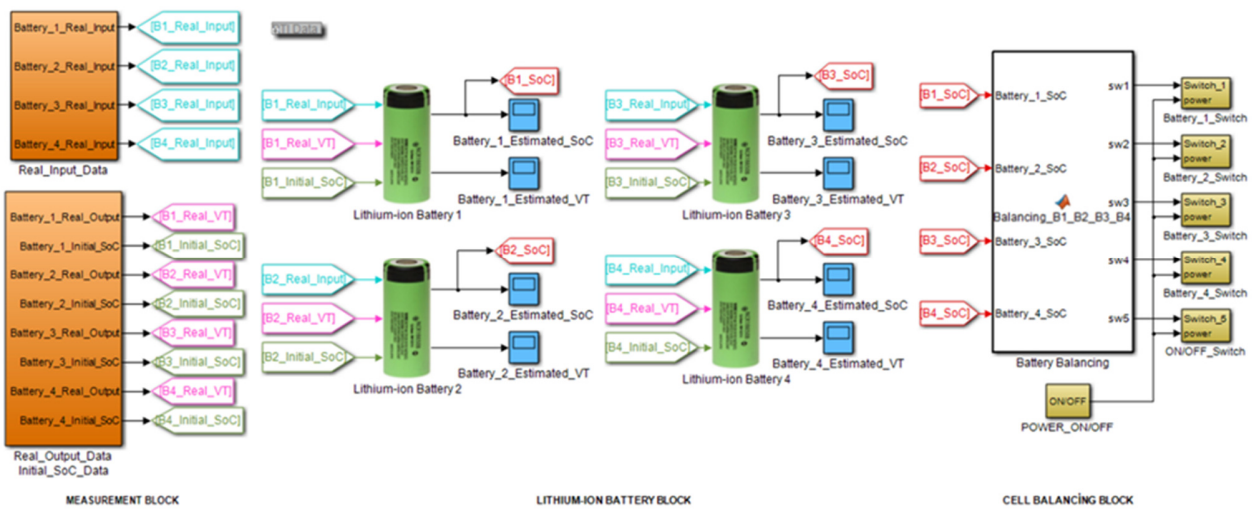


Fig. 9 Matlab interface of the equalization process

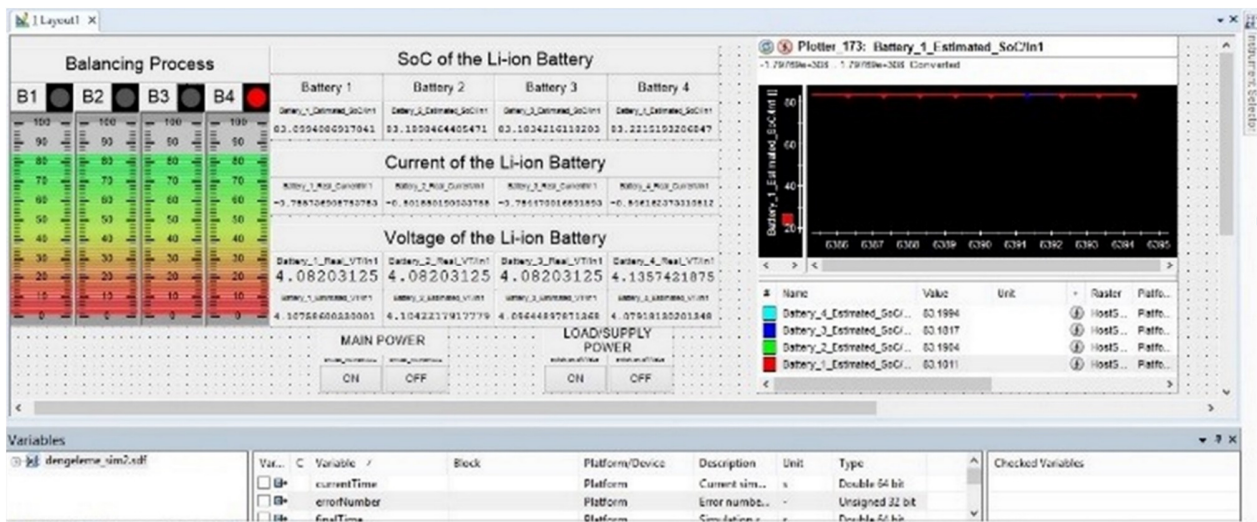


Fig. 10 Graphical user interface of the equalization process

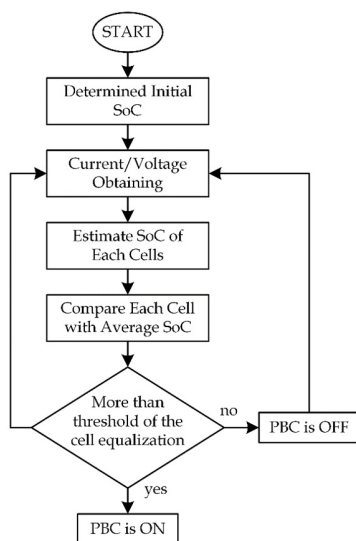


Fig. 11 Algorithm of the equalization process

D. Validation of PBC

The PBC is applied to four series of Li-ion cells to test and verify the presented equalization scheme.

In the first experiment, the battery pack is discharged at the load current which is randomly varied between 0.65A and 1A. To examine the performance of the balancing process, the PBC is turned off after 180min. The result of the first experiment is shown in Figure 12. In the second experiment, the balanced battery cells are charged for 180s. Afterwards, only the PBC of B1 cell (first battery cell) is turned off during the charging process. Unbalanced battery cells are charged for 320s and afterwards the PBC of the B1 cell is turned on for balancing in the discharge process. When the cells are equalized, the PBC of the B1 cell is turned off again during the charging process for 600s. Then the PBC of B1 cell is turned on for balancing in the charge process until the cells are equalized. The result of the second experiment is shown in Figure 13. As shown in Figure 12, cell inconsistencies were successfully prevented during discharge process until the PBC was off. On the other hand,

cell inconsistencies were quickly observed when the PBC was turned off. Likewise, it was seen that the unbalanced cells equalize rapidly during both charging and discharging processes as shown in Figure 13. Experimental results validate that PBC can equalize the Li-ion cells accurately and rapidly by using UKF-based estimation with combined dynamic battery model.

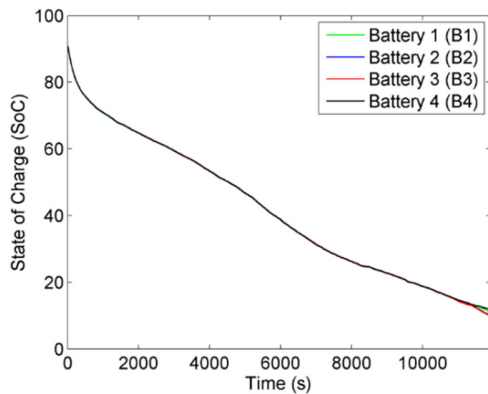


Fig. 12 SoC vs time, first experiment

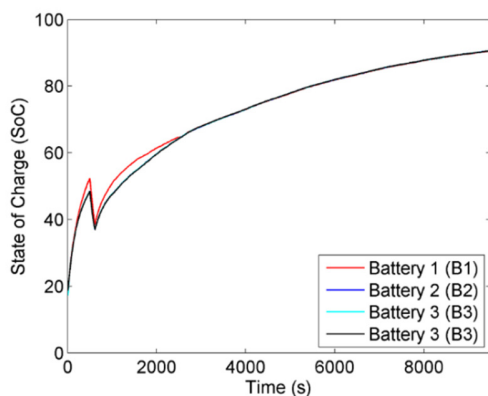


Fig. 13 SoC vs time, second experiment

VI. CONCLUSION

This paper presented a SoC based equalization scheme based on PBC. A combined dynamic model of the Li-ion battery was proposed by using a second order Thevenin model, OCV, and CC method. In the combined dynamic model, the parameters of the equivalent circuit vary depending on SoC. Accurate SoC estimation of each Li-ion cell was implemented by UKF. The SoC based equalization utilizing PBC was applied to equalization of the unbalanced of series-connected Li-ion batteries. The simulation architecture utilizing PBC was designed in MATLAB/Simulink. Real-time experimental verification was performed with a real-time controller Dspace DS1104. Two different experiments were performed to validate the effect of the designed PCB unit. In the first experiment, the battery pack was discharged under variable loads and cell imbalance was successfully prevented by the PCB unit during the discharge process. In the second experiment, the battery pack was tested under the charge/discharge conditions at different times and unbalanced cells equalized rapidly during

charging and discharging process. The experimental results show that the presented PCB based equalization scheme and UKF based SoC estimation can perform well in real-time applications.

ACKNOWLEDGMENT

The authors would like to thank the Scientific and Technological Research Council of Turkey (TÜBİTAK-3501, 114E515) for the financial support.

REFERENCES

- [1] M. A. Hannan, M. S. H. Lipu, A. Hussain, A. Mohamed, "A review of lithium-ion battery state of charge estimation and management system in electric vehicle applications: Challenges and recommendations", *Renewable and Sustainable Energy Reviews*, Vol. 78, pp. 834-854, 2017
- [2] V. H. M. Nguyen, C. V. Vo, L. D. L. Nguyen, B. T. T. Phan, "Green scenarios for power generation in Vietnam by 2030", *Engineering, Technology & Applied Science Research*, Vol. 9, No. 2, pp. 4019-4026, 2019
- [3] E. V. Palconit, M. L. S. Abundo, "Transitioning to green maritime transportation in Philippines: Mapping of potential sites for electric ferry operations", *Engineering, Technology & Applied Science Research*, Vol. 9, No. 1, pp. 3770-3773, 2019
- [4] G. E. Blomgren, "The development and future of lithium ion batteries", *Journal of the Electrochemical Society*, Vol. 164, No. 1, pp. A5019-A5025, 2017
- [5] X. Hu, C. Zou, C. Zhang, Y. Li, "Technological developments in batteries: A survey of principal roles, types, and management needs", *IEEE Power and Energy Magazine*, Vol. 15, No. 5, pp. 20-31, 2017
- [6] P. Shen, M. Ouyang, L. Lu, J. Li, X. Feng, "The co-estimation of state of charge, state of health, and state of function for lithium-ion batteries in electric vehicles", *IEEE Transactions on Vehicular Technology*, Vol. 67, No. 1, pp. 92-103, 2018
- [7] X. Wang, J. Xu, Y. Zhao, "Wavelet based denoising for the estimation of the state of charge for lithium-ion batteries", *Energies*, Vol. 11, No. 5, pp. 1144, 2018
- [8] L. Lu, X. Han, J. Li, J. Hua, M. Ouyang, "A review on the key issues for lithium-ion battery management in electric vehicles", *Journal of Power Sources*, Vol. 226, pp. 272-288, 2013
- [9] A. Fotouhi, D. J. Auger, K. Propp, S. Longo, M. Wild, "A review on electric vehicle battery modelling: from lithium-ion toward lithium-sulphur", *Renewable and Sustainable Energy Reviews*, Vol. 56, pp. 1008-1021, 2016
- [10] X. Lai, Y. Zheng, T. Sun, "A comparative study of different equivalent circuit models for estimating state-of-charge of lithium-ion batteries", *Electrochimica Acta*, Vol. 259, pp. 566-577, 2018
- [11] C. Zhang, W. Allafi, Q. Dinh, P. Ascencio, J. Marco, "Online estimation of battery equivalent circuit model parameters and state of charge using decoupled least squares technique", *Energy*, Vol. 142, pp. 678-688, 2018
- [12] R. Xiong, J. Cao, Q. Yu, H. He, F. Sun, "Critical review on the battery state of charge estimation methods for electric vehicles", *IEEE Access*, Vol. 6, pp. 1832-1843, 2017
- [13] R. Zhang, B. Xia, B. Li, L. Cao, Y. Lai, W. Zheng, "State of the art of lithium-ion battery SOC estimation for electrical vehicles", *Energies*, Vol. 11, No. 7, pp. 1820, 2018
- [14] Y. Zheng, M. Ouyang, X. Han, L. Lu, J. Li, "Investigating the error sources of the online state of charge estimation methods for lithium-ion batteries in electric vehicles", *Journal of Power Sources*, Vol. 377, pp. 161-188, 2018
- [15] W. Y. Chang, "The state of charge estimating methods for battery: A review", *ISRN Applied Mathematics*, Vol. 2013, Article ID 953792, 2013
- [16] N. C. Eli-Chukwu, "Applications of artificial intelligence in agriculture: A review", *Engineering, Technology & Applied Science Research*, Vol. 9, No. 4, pp. 4377-4383, 2019

- [17] K. S. Ng, Y. F. Huang, C. S. Moo, Y. C. Hsieh, "An enhanced coulomb counting method for estimating state-of-charge and state-of-health of lead-acid batteries", 31st International Telecommunications Energy Conference, Incheon, South Korea, October 18-22, 2009
- [18] S. Wang, C. Fernandez, L. Shang, Z. Li, H. Yuan, "An integrated online adaptive state of charge estimation approach of high-power lithium-ion battery packs", Transactions of the Institute of Measurement and Control, Vol. 40, No. 6, pp. 1892-1910, 2017
- [19] C. Zhang, J. Jiang, L. Zhang, S. Liu, L. Wang, P. C. Loh, "A generalized SOC-OCV model for lithium-ion batteries and the SOC estimation for LNMCO battery", Energies, Vol. 9, No. 11, Article ID 900, 2016
- [20] L. Lavigne, J. Sabatier, J. M. Francisco, F. Guillemard, A. Noury, "Lithium-ion open circuit voltage (OCV) curve modelling and its ageing adjustment", Journal of Power Sources, Vol. 324, pp. 694-703, 2016
- [21] M. Charkhgard, M. Farrokhi, "State-of-charge estimation for lithium-ion batteries using neural networks and EKF", IEEE Transactions on Industrial Electronics, Vol. 57, No. 12, pp. 4178-4187, 2010
- [22] L. Xu, J. Wang, Q. Chen, "Kalman filtering state of charge estimation for battery management system based on a stochastic fuzzy neural network battery model", Energy Conversion and Management, Vol. 53, No. 1, pp. 33-39, 2012
- [23] G. Burgers, P. J. V. Leeuwen, G. Evensen, "Analysis scheme in the ensemble Kalman filter", Monthly Weather Review, Vol. 126, No. 6, pp. 1719-1724, 1998
- [24] O. Aydogdu, M. L. Levent, "Kalman state estimation and LQR assisted adaptive control of a variable loaded servo system", Engineering, Technology & Applied Science Research, Vol. 9, No. 3, pp. 4125-4130, 2019
- [25] K. Fujii, Extended Kalman filter, The ACFA-Sim-J Group, 2013
- [26] F. Claude, M. Becherif, H. S. Ramadan, "Experimental validation for lithium battery modeling using extended Kalman filters", International Journal of Hydrogen Energy, Vol. 42, No. 40, pp. 25509-25517, 2017
- [27] S. Jung, H. Jeong, "Extended Kalman filter-based state of charge and state of power estimation algorithm for unmanned aerial vehicle li-po battery packs", Energies, Vol. 10, No. 8, pp. 1237, 2017
- [28] M. Mathew, S. Janhunnen, M. Rashid, F. Long, M. Fowler, "Comparative analysis of lithium-ion battery resistance estimation techniques for battery management systems", Energies, Vol. 11, No. 6, pp. 1490, 2018
- [29] E. A. Wan, R. V. D. Merwe, "The unscented Kalman filter for nonlinear estimation", Adaptive Systems for Signal Processing, Communications, and Control Symposium, Alberta, Canada, October 4, 2000
- [30] Y. He, X. Liu, C. Zhang, Z. H. Chen, "A new model for state-of-charge (SOC) estimation for high-power li-ion batteries", Applied Energy, Vol. 101, pp. 808-814, 2013
- [31] W. He, N. Williard, C. Chen, M. Pecht, "State of charge estimation for electric vehicle batteries using unscented Kalman filtering", Microelectronics Reliability, Vol. 53, No. 6, pp. 840-847, 2013
- [32] H. He, H. Qin, X. Sun, Y. Shui, "Comparison study on the battery SoC estimation with EKF and UKF algorithms", Energies, Vol. 6, No. 10, pp. 5088-5100, 2013
- [33] S. Peng, C. Chen, H. Shi, Z. Yao, "State of charge estimation of battery energy storage systems based on adaptive unscented Kalman filter with a noise statistics estimator", IEEE Access, Vol. 5, pp. 13202-13212, 2017
- [34] Y. Ma, P. Duan, Y. Sun, H. Chen, "Equalization of lithium-ion battery pack based on fuzzy logic control in electric vehicle", IEEE Transactions on Industrial Electronics, Vol. 65, No. 8, pp. 6762-6771, 2018
- [35] D. D. Quinn, T. T. Hartley, "Design of novel charge balancing networks in battery packs", Journal of Power Sources, Vol. 240, pp. 26-32, 2013
- [36] Y. Zheng, L. Lu, X. Han, J. Li, M. Ouyang, "LiFePO₄ battery pack capacity estimation for electric vehicles based on charging cell voltage curve transformation", Journal of Power Sources, Vol. 226, pp. 33-41, 2013
- [37] Y. Li, C. Wang, J. Gong, "A combination Kalman filter approach for state of charge estimation of lithium-ion battery considering model uncertainty", Energy, Vol. 109, pp. 933-946, 2016